PHYSICAL REVIEW C **81**, 021304(R) (2010)

Interpretation of Coulomb breakup of ^{31}Ne in terms of deformation

Ikuko Hamamoto
Division of Mathematical Physics, Lund Institute of Technology at the University of Lund, Lund, Sweden and The Niels Bohr Institute, Blegdamsvej 17, Copenhagen Ø, DK-2100, Denmark
(Received 12 December 2009; published 23 February 2010)

The recent experimental data on Coulomb breakup of the nucleus ^{31}Ne are interpreted in terms of deformation. The measured large one-neutron removal cross section indicates that the ground state of ^{31}Ne is either an s halo or a p halo. The data can be most easily interpreted as the spin of the ground state being $3/2^-$ coming from either the Nilsson level [330 1/2] or the Nilsson level [321 3/2] depending on the neutron separation energy S_n. However, the possibility of $1/2^+$ coming from [200 1/2] is not excluded. It is suggested that if the large ambiguity in the measured value of S_n of ^{31}Ne, 0.29 ± 1.64 MeV, can be reduced by an order of magnitude, say to be ± 100 keV, one may get a clear picture of the spin-parity of the halo ground state.

DOI: 10.1103/PhysRevC.81.021304 PACS number(s): 21.10.Gv, 21.10.Jx, 21.10.Pc, 27.30.+t

Recent experimental data obtained by using radioactive ion beams reveal that the neutron numbers such as $N = 8$, 20, and 28 are no longer magic numbers in some nuclei toward the neutron drip line. Those neutron-rich nuclei can well be interpreted as being deformed and are often called nuclei in the island of inversion. One-neutron removal cross sections of a very-neutron-rich nucleus ^{31}Ne due to the Coulomb breakup are reported in Ref. [1] and found to provide evidence of the soft $E1$ excitation. The analysis of the cross section in Ref. [1] is based on one-particle wave functions in the spherical Woods-Saxon potential. It was concluded that the measured large one-neutron removal cross sections were consistent with a $p_{3/2}$ or $s_{1/2}$ neutron halo when a spectroscopic factor considerably smaller than unity was introduced. The heaviest halo nucleus so far experimentally established is ^{19}C with the ground-state spin of $1/2^+$, namely, an s-halo nucleus. While the nucleus ^{19}C may be interpreted as a spherical halo nucleus, the data on ^{31}Ne in Ref. [1] may be most easily interpreted in terms of the deformation or the one-particle motion in the deformed mean field, since the spin-parity of the halo ground state cannot be $7/2^-$, which is expected for the 21st neutron for spherical shape. We note that the analysis of the spectroscopic data on light mirror nuclei, $^{25}_{12}$Mg$_{13}$ and $^{25}_{13}$Al$_{12}$, is successfully performed in Ref. [2] in terms of the deformed mean field using Nilsson orbits occupied by the 13th nucleon. In the present rapid communication we attempt the interpretation of the data in Ref. [1] based on a deformed mean field, using one-particle neutron wave functions obtained by properly taking into account the weak binding.

The measured low-excitation energies of the first 2^+ state of both ^{30}Ne [3] and ^{32}Ne [4] are consistent with the picture that the Ne isotope with these neutron numbers lies inside the island of inversion. Moreover, the large Coulomb breakup cross section reported in Ref. [1], which clearly indicates the halo nature of the ground state of ^{31}Ne, suggests the efficient contribution by an s or p component of the 21st neutron in the deformed mean field. These observations invite us to carry out the analysis of the data on ^{31}Ne in terms of deformation. It should be also noted that the measured spin and magnetic moments of the ground state of $^{33}_{12}$Mg$_{21}$, which have the same neutron number $N = 21$, are reported in Ref. [5] and are consistent with the interpretation of $I^\pi = 3/2^-$, while both neighboring even-even nuclei, ^{32}Mg and ^{34}Mg, are well interpreted as being deformed. However, since the neutron separation energy of $^{33}_{12}$Mg$_{21}$ is 2.22 MeV, a neutron halo is not expected.

Low-lying states of odd-A medium-heavy deformed nuclei are in a good approximation expressed by one (quasi)particle moving in the deformed field produced by the even-even core [2]. A one-particle picture works much better in deformed nuclei than in spherical nuclei, because the major part of the long-range residual interaction in the spherical mean field can be included in the deformed mean field. In contrast, when the spherical shell model is applied to nuclei in the island of inversion, the resultant wave functions are not easy to predict due to the complicated configuration mixing. Furthermore, since harmonic-oscillator wave functions are always used in the traditional shell model calculations, the applicability of the calculations to the description of halo nuclei can be questioned.

We start with our formulation for spherical shape. The neutron bound-state wave function is an eigenfunction of the Woods-Saxon potential with an energy eigenvalue $\varepsilon < 0$,

$$\left|\Phi^{(b)}_{\varepsilon} : \ell j m\right\rangle = \frac{1}{r} R^{(b)}_{n\ell j}(\varepsilon, r)[Y_\ell \otimes \chi_{1/2}]_{jm}, \tag{1}$$

where

$$R^{(b)}_{n\ell j}(\varepsilon, r) \propto \alpha r\, h_\ell(\alpha r), \tag{2}$$

with

$$h_\ell(-iz) \equiv j_\ell(z) + i n_\ell(z), \tag{3}$$

$$\alpha^2 = -\frac{2\mu\varepsilon}{\hbar^2}, \tag{4}$$

$$\int_0^\infty dr \left|R^{(b)}_{n\ell j}(\varepsilon, r)\right|^2 = 1. \tag{5}$$

We choose to express one-particle neutron wave functions in the continuum using the real energy variable $\varepsilon > 0$,

$$\left|\Phi_{\varepsilon}^{(c)} : \ell j m\right\rangle = \frac{1}{r} R_{\ell j}^{(c)}(\varepsilon, r)[Y_\ell \otimes \chi_{1/2}]_{jm} \tag{6}$$

$$= \sqrt{\frac{2\mu}{\hbar^2 \pi k}} [\cos(\delta_{\ell j})\, k\, j_\ell(kr) - \sin(\delta_{\ell j})\, k\, n_\ell(kr)] \times [Y_\ell \otimes \chi_{1/2}]_{jm}, \tag{7}$$

where μ expresses the reduced mass and

$$k^2 = \frac{2\mu\varepsilon}{\hbar^2}, \tag{8}$$

while the normalization is expressed as

$$\int_0^\infty dr\, R_{\ell j}^{(c)}(\varepsilon, r) R_{\ell j}^{(c)}(\varepsilon', r) = \delta(\varepsilon - \varepsilon'). \tag{9}$$

The $B(E1)$ value of the $E1$ excitation from a bound one-particle (j_b) level to a continuum one-particle (j_c) level keeping the even-even core in the ground state as a spectator is written as

$$\frac{dB[E1, b(j_b) \to c(j_c)]}{dE} = (Z_{\rm eff} e)^2 \frac{2j_c + 1}{4\pi} \left[C\left(j_c, j_b, 1; \frac{1}{2}, \frac{-1}{2}, 0\right)\right]^2 \times \left| \int r dr\, R_{j_b}^{(b)}(\varepsilon_b, r) R_{j_c}^{(c)}(\varepsilon_c, r)\right|^2. \tag{10}$$

First, it is found that the Coulomb breakup by the soft $E1$ excitation of halo neutrons occurs far outside the nucleus ^{31}Ne, noting that no one-particle resonance with the relevant angular momentum is present in the low-energy continuum. In Fig. 1 we plot the $2p_{3/2}$ radial wave function with the eigenenergy $\varepsilon_b = -300$ keV, the continuum $s_{1/2}$ radial wave function with $\varepsilon_c = +60$ keV, and the product of those two wave functions multiplied by the radial variable. The value of ε_c is chosen as an example, because for $\varepsilon_b = -300$ keV the quantity in Eq. (10) reaches the maximum around $\varepsilon_c = +60$ keV [6]. From Fig. 1 it is seen that the major part of the soft $E1$ matrix element comes from the region of $r = 8$–40 fm, far outside of the core nucleus ^{30}Ne. A similar result is obtained also for soft $E1$ excitations of the halo p neutron to continuum d levels, though the Coulomb breakup cross section is much smaller than that of the excitation to s levels. Both the tail shape and the amplitude of the wave function of the halo neutron are very important for the cross sections of the Coulomb breakup, while the wave functions inside ^{31}Ne may hardly play a role.

In the phenomena where the structure of deformed wave functions plays a role, the expression in Eq. (10) is replaced by the reduced matrix element in Eqs. (4-91) of Ref. [2] together with Eqs. (1A-67) of Ref. [7]. Continuum one-particle wave functions in a deformed mean field are calculated in terms of eigenphase [8,9]. For given ε_c and Ω^π values there are a number of independent one-particle wave functions, the number of which is equal to that of eigenphases, and all possible contributions must be calculated and summed up. However, when soft $E1$ excitations that produce such large Coulomb breakup cross sections as those in Ref. [1] should

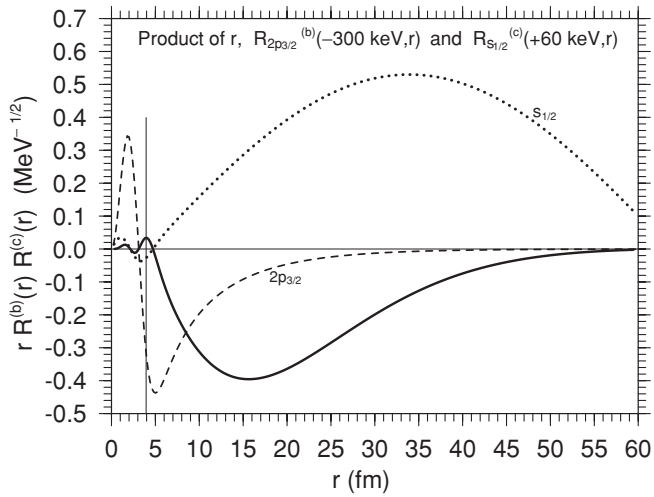

FIG. 1. The integrand of the radial integral on the right-hand side of Eq. (10) as a function of radial variable r. Namely, the product (solid curve) of radial variable, the bound $2p_{3/2}$ radial wave function $R_{2p_{3/2}}^{(b)}$ ($\varepsilon = -300$ keV, r) (dashed curve) in units of fm$^{-1/2}$, and the continuum $s_{1/2}$ radial wave function $R_{s_{1/2}}^{(c)}$ ($\varepsilon = +60$ keV, r) (dotted curve) in units of fm$^{-1/2}$ MeV$^{-1/2}$. The unit of the ordinate is for the product, while the figures written along the ordinate can be used also for the radial wave functions, $R_{2p_{3/2}}^{(b)}$ and $R_{s_{1/2}}^{(c)}$, in respective units. The radial integration of the solid curve gives the radial matrix element of the $E1$ transition, $2p_{3/2} \to s_{1/2}$. The depth of the Woods-Saxon potential is -46.75 MeV for which the eigenstate of the $2p_{3/2}$ neutron is obtained at -300 keV, while the diffuseness and the radius used are 0.67 and 3.946 fm (for $A = 30$), respectively.

be estimated, we may conveniently use the halo one-neutron wave function taken from the s or p component of deformed Nilsson levels (an approximation in terms of "spectroscopic factor"), while one-particle wave functions in the continuum are estimated for the spherical part of the Woods-Saxon potential.

In Fig. 2, the Nilsson diagram is shown, of which the parameters are approximately adjusted to the (^{30}Ne + n) system. The calculation was done in the same manner as in Ref. [10]. At $\beta = 0$ the $1f_{7/2}$ one-neutron resonance is found at 2.40 MeV with the width of 0.224 MeV, while neither the $2p_{3/2}$ nor the $2p_{1/2}$ resonance defined by the eigenphase formalism [8,9] is obtained. However, the complicated nonlinear behavior of the [330 1/2] resonant level for $0.1 < \beta < 0.2$ in the continuum (denoted by a dotted curve) indicates that the resonantlike component with $\Omega^\pi = 1/2^-$ coming from $2p_{3/2}$ is present around the energy region. Indeed the $2p_{3/2}$ resonance lying lower than the $1f_{7/2}$ one is found if we use a slightly more attractive Woods-Saxon potential. For the parameters used in Fig. 2 the Nilsson level that is to be occupied by the 21st neutron is [330 1/2] for $0.22 \lesssim \beta \lesssim 0.30$, [202 3/2] for $0.30 \lesssim \beta \lesssim 0.40$, [321 3/2] for $0.40 \lesssim \beta \lesssim 0.59$, and [200 1/2] for $\beta \gtrsim 0.59$. Varying the parameters of the one-body potential within a reasonable range, any Nilsson levels other than those four levels are hardly obtained for the 21st neutron. The spin-parity of the lowest state is $I^\pi = 3/2^-$ for [330 1/2] due to the decoupling parameter lying between -2 (for $p_{3/2}$) and -4 (for the $f_{7/2}$), $3/2^+$ for [202 3/2], $3/2^-$ for [321

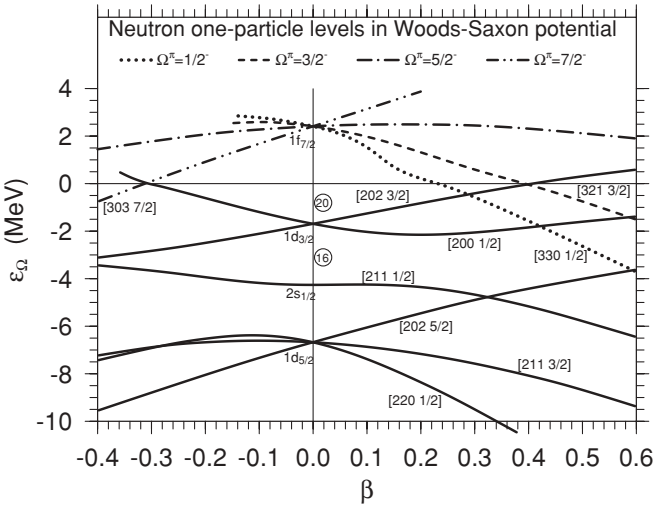

FIG. 2. Neutron one-particle levels in Woods-Saxon potentials as a function of quadrupole deformation parameter β. The potential depth is approximately adjusted so that the 21st neutron of the prolately deformed nucleus ^{31}Ne can be a halo neutron. The depth, the diffuseness and the radius of the potential are -39 MeV, 0.67 fm, and 3.946 fm (for $A = 30$), respectively. Positive-parity levels are plotted by solid curves, while asymptotic quantum numbers [N n_z Λ Ω] are denoted for bound levels. See the text for details.

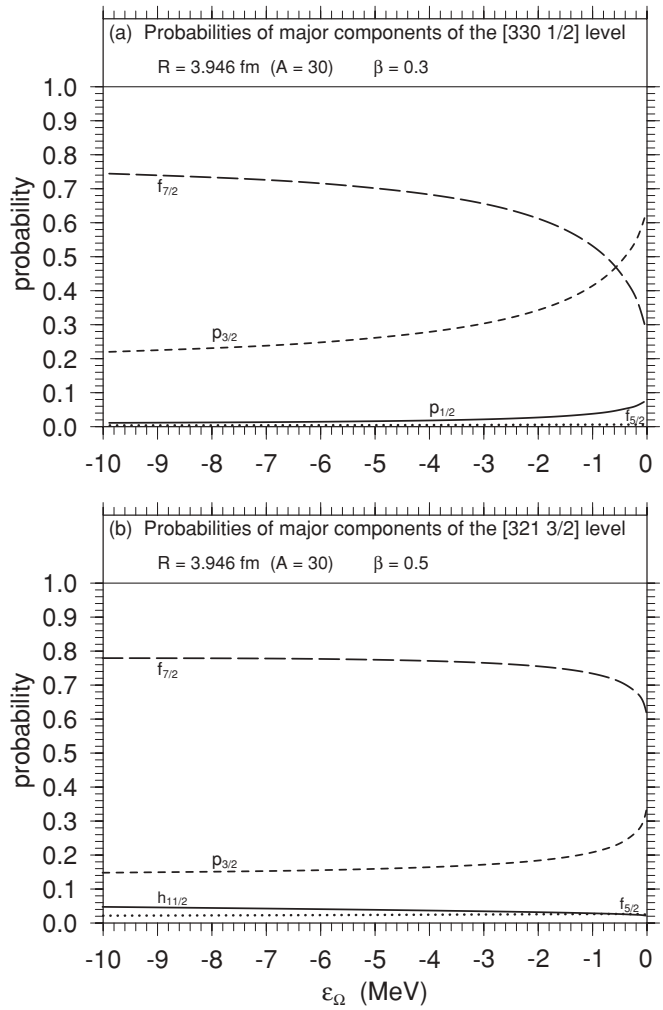

FIG. 3. (a) Calculated probabilities of the major components of the [330 1/2] level with $\beta = 0.3$ as a function of energy eigenvalue ε_Ω. (b) Calculated probabilities of the major components of the [321 3/2] level with $\beta = 0.5$ as a function of energy eigenvalue ε_Ω. The potential depth is adjusted to obtain respective ε_Ω values as energy eigenvalues of the deformed potential. The diffuseness and the radius of the potential are 0.67 and 3.946 fm (for $A = 30$), respectively.

3/2], and $1/2^+$ for [200 1/2]. Among those four Nilsson orbitals the [202 3/2] level is excluded as a candidate for the configuration of the ground state of ^{31}Ne, because the smallest orbital-angular-momentum in the wave function of [202 3/2] is $\ell = 2$, which makes very little halo. Examining Fig. 2 we may also note that the presence of ^{31}Ne inside the neutron drip line is possibly realized by the deformation which is created by the Jahn-Teller effect due to the near degeneracy of $1f_{7/2}$, $2p_{3/2}$, and $2p_{1/2}$ shells in the continuum for spherical shape.

In Figs. 3(a) and 3(b) the probabilities of appreciable components of the [330 1/2] and [321 3/2] levels calculated at $\beta = 0.3$ and 0.5, respectively, are shown, while the channels of $p_{1/2}$ (only in [330 1/2]), $p_{3/2}$, $f_{5/2}$, $f_{7/2}$, $h_{9/2}$, and $h_{11/2}$ are included in the calculation. The radius of the Woods-Saxon potential is fixed, while the depth is adjusted so as to obtain respective Nilsson levels as eigenstates of the deformed potential. As shown in Refs. [11,12], the p components in $\Omega^\pi = 1/2^-$ and $3/2^-$ Nilsson levels increase as the binding energies approach zero, though the probabilities at zero energies depend on Nilsson levels. This is in contrast to the fact that the probability of the s component in $\Omega^\pi = 1/2^+$ Nilsson levels becomes always unity as the binding energy approaches zero. For example, at $\varepsilon_\Omega = -300$ keV the probability of the $p_{3/2}$ component in the [330 1/2] level for $\beta = 0.3$ and the [321 3/2] level for $\beta = 0.5$ is 0.5225 and 0.2534, respectively. For reference, at $\varepsilon_\Omega = -300$ keV the probability of the $s_{1/2}$ component in the [200 1/2] level for $\beta = 0.5$ is 0.67.

Now, for example, the shape of the radial wave function of the $p_{3/2}$ component of [330 1/2] at $\beta = 0.3$ is not the same as that of the bound $2p_{3/2}$ level, even if both [330 1/2] and $2p_{3/2}$ levels are calculatd at the same energy, because the latter is an eigenstate of a given spherical potential while the former is not. Moreover, two different spherical potentials lead to different radial wave functions of $s_{1/2}$ at a given energy in the continuum. These differences may induce a nonnegligible change in the resulting $B(E1)$ values, even after the normalization of the $2p_{3/2}$ wave function is adjusted to be the same as the probability of the $p_{3/2}$ component in [330 1/2]. In Fig. 4 we show the squared radial integral on the right-hand side of Eq. (10) as a function of the continuum $s_{1/2}$ energy ε_c, which is calculated using the following two kinds of $p_{3/2}$ bound-state wave functions: (i) the $2p_{3/2}$ wave function with the energy eigenvalue -300 keV for a spherical potential and a normalization of 0.5225; (ii) the $p_{3/2}$ component of [330 1/2] which has the energy of -300 keV in the deformed potential with $\beta = 0.3$. The difference between the two radial wave functions, $2p_{3/2}$ in (i) and $p_{3/2}$ in (ii), disappears quickly outside the nuclear radius. The appreciable difference in $dB(E1)/dE$ values of the two cases appears only for small ε_c values, and the integration of the two curves over ε_c up till

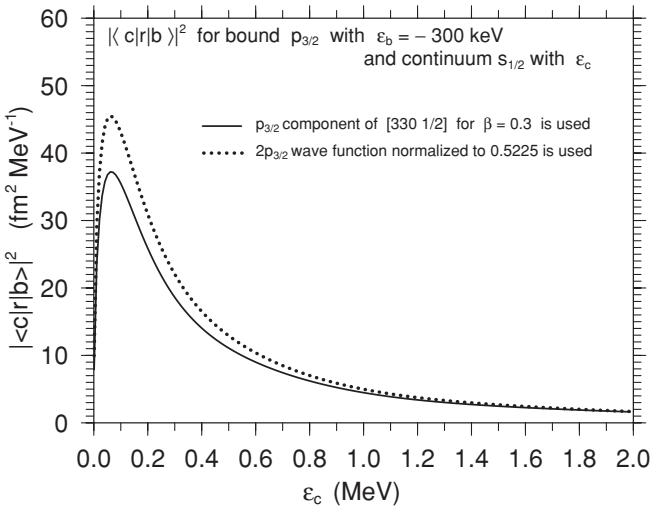

FIG. 4. Estimate of $|\int r\,dr\, R^{(b)}_{p_{3/2}}(-300\ \text{keV}, r)\, R^{(c)}_{s_{1/2}}(\varepsilon_c, r)|^2$ on the right-hand side of Eq. (10) as a function of ε_c. The solid curve is obtained by using the $p_{3/2}$ wave function taken from the $p_{3/2}$ component of the [330 1/2] level, which is bound at -300 keV for $\beta = 0.3$. The probability of the $p_{3/2}$ component is 0.5225. The dotted curve is calculated using the $2p_{3/2}$ wave function with the energy eigenvalue -300 keV, which is normalized to 0.5225. The depth of the Woods-Saxon potential of the former is -38.39 MeV, while that of the latter is -46.75 MeV.

2 MeV gives a difference of about 15%. Generally speaking, if we replace the $p_{3/2}$ component of the [330 1/2] level or the [321 3/2] level by the $2p_{3/2}$ wave function with the same neutron binding and normalization, the $E1$ transition $2p_{3/2} \rightarrow s_{1/2}$ has a larger $B(E1)$ value than that of $p_{3/2} \rightarrow s_{1/2}$. "Larger" or "smaller" depends on whether the spherical $(2p_{3/2})$ eigenstate lies energetically higher or lower than the one-particle level in the Nilsson diagram for the relevant value of $\beta \neq 0$. The larger the energy difference, the larger the difference in the $B(E1)$ values appears, which comes from the different radial shape of the two wave functions.

By combining Figs. 3(a) and 3(b) with Fig. 2 of Ref. [1], for a given S_n value we may find the relevant Nilsson level and the spin-parity of the ground state of the halo nucleus ^{31}Ne, which are consistent with the observed Coulomb breakup cross section. It is noted that the strong ε_b dependence of the radial integral in Eq. (10) coming from the weakly bound $p_{3/2}$ or $s_{1/2}$ neutron wave function is already taken care of in Fig. 2 of Ref. [1]. After taking into account both possible ambiguities in the parameters of the one-body potential and the approximation in terms of the "spectroscopic factor" of s or p neutrons, we may conclude at least the following; The ground state has $I^\pi = 1/2^+$ coming from the Nilsson level [200 1/2] if S_n is appreciably larger than 500 keV. In this case the relevant deformation is expected to be very large, $\beta \gtrsim 0.6$. If S_n is smaller than 500 keV, the ground state can be a p-wave halo and $I^\pi = 3/2^-$. If S_n is smaller than 200 keV, the relevant Nilsson level may be [321 3/2]. Otherwise, it is [330 1/2].

Improving the accuracy of the measured S_n value to much better than that of the available value [13], $S_n = 0.29 \pm 1.64$ MeV, can clarify the I^π value when it is combined with the data in Ref. [1]. On the other hand, for example, the measurement of the magnetic moment of ^{31}Ne may not clearly pin down the spin-parity, since the estimated magnetic moment coming from the $N = 21$st neutron in a deformed core is anyway negative and lies in the range of $-0.4 \lesssim \mu/\mu_N \lesssim -1.0$ for possible states with $I^\pi = 3/2^-$ coming from either [330 1/2] or [321 3/2] Nilsson orbits and those with $I^\pi = 1/2^+$ from [200 1/2].

In the present analysis the possibility of excited states of ^{30}Ne after the Coulomb breakup is not included; however, the related Coulomb breakup cross section is relatively small and lies within the ambiguities in the model calculation. The possible many-body pair correlation is not included either. This is because, first of all, the halo neutron wave-function extends so much beyond the core nucleus that it couples weakly to the pairing field provided by the well-bound core nucleons. Second, in the ground state of odd-N nuclei the relevant neutron single-particle energy lies very close to the Fermi level. Then, irrespective of the nature of one-particle orbits, the occupation probability of the doubly degenerate neutron level obtained from solving the Hartree-Fock-Bogoliubov equation is approximately equal to 0.5 [14,15]. Therefore, the contribution of halo neutrons to the Coulomb breakup which is estimated in the present article is expected to work as a first approximation.

In conclusion, it is shown that the observed large Coulomb breakup cross section of ^{31}Ne in Ref. [1] is interpreted most easily and simply in terms of p-wave neutron halo together with the deformed core ^{30}Ne. The measurement of S_n with an accuracy much better than that of the presently available one will clarify the spin-parity of the ground state of ^{31}Ne.

Fruitful discussions with Professor T. Nakamura are much appreciated.

[1] T. Nakamura *et al.*, Phys. Rev. Lett. **103**, 262501 (2009).
[2] A. Bohr and B. R. Mottelson, *Nuclear Structure* (Benjamin, Reading, MA, 1975), Vol. II.
[3] Y. Yanagisawa *et al.*, Phys. Lett. **B566**, 84 (2003).
[4] P. Doornenbal *et al.*, Phys. Rev. Lett. **103**, 032501 (2009).
[5] D. T. Yordanov *et al.*, Phys. Rev. Lett. **99**, 212501 (2007).
[6] M. A. Nagarajan, S. M. Lenzi, and A. Vitturi, Eur. Phys. J. A **24**, 63 (2005).
[7] A. Bohr and B. R. Mottelson, *Nuclear Structure* (Benjamin, Reading, MA, 1969), Vol. I.
[8] I. Hamamoto, Phys. Rev. C **72**, 024301 (2005).
[9] I. Hamamoto, Phys. Rev. C **73**, 064308 (2006).
[10] I. Hamamoto, Phys. Rev. C **76**, 054319 (2007).
[11] T. Misu, W. Nazarewicz, and S. Åberg, Nucl. Phys. **A614**, 44 (1997).
[12] I. Hamamoto, Phys. Rev. C **69**, 041306(R) (2004).
[13] B. Jurado *et al.*, Phys. Lett. **B649**, 43 (2007).
[14] I. Hamamoto and B. R. Mottelson, Phys. Rev. C **68**, 034312 (2003).
[15] I. Hamamoto, Phys. Rev. C **73**, 044317 (2006).